J Oral Pathol Med (2004) 33: 79–86

www.blackwellmunksgaard.com/jopm

Establishment of OC3 oral carcinoma cell line and identification of NF-κB activation responses to areca nut extract

Shu-Chun Lin[1], Chung-Ji Liu[1,3], Chun-Po Chiu[1], Shun-Ming Chang[1], Suu-Yi Lu[1], Yann-Jang Chen[2]

[1]*School of Dentistry,* [2]*Department of Life Science, National Yang-Ming University, and* [3]*Department of Dentistry, Mackay Memorial Hospital, Taipei, Taiwan*

BACKGROUND: Cell lines derived from oral squamous cell carcinoma (OSCC) exposed to variable etiological factors can bestow advantages in understanding the molecular and cellular alterations pertaining to environmental impacts. Most OSCC cell lines have been established from smoker patients or areca chewing/smoker patients, carrying the genomic alterations in *p53*.
METHODS: A new cell line, oral carcinoma 3 (OC3), was established from an OSCC in a long-term areca (betel) chewer who does not smoke. Cellular and molecular features of OC3 were determined by variable assays.
RESULTS: The cultured monolayer cells were mainly polygonal and had the expression of cytokeratin 14. The chromosomal analysis using comparative genomic hybridization has revealed the gain in chromosomes 1q, 5q, and 8q, the loss in 4q, 6p, and 8p as well as the gain of entire chromosome 20. Loss of heterozygosity and instability in multiple microsatellite markers in chromosome 4q were also noted. OC3 cells bear wild-type *p53* coding sequence and have a high level of p53 expression. Its p21 expression was similar to that in normal human oral keratinocyte (NHOK). Interestingly, activation of nuclear factor κB (NF-κB) in OC3 cells following the treatment of areca nut extract was observed.
CONCLUSION: OC3 cell line could be valuable in understanding the genetic impairments and phenotypic changes associated with areca in oral keratinocyte.
J Oral Pathol Med (2004) **33**: 79–86

Keywords: areca; mouth neoplasm; NF-κB; p53; 4q

Introduction

Oral squamous cell carcinoma (OSCC) is a common malignancy worldwide. It was etiologically linked to tobacco use, areca (betel) chewing, alcohol consumption, and, etc. The high incidence of OSCC in South-east or South Asia is specifically related to combined areca chewing/tobacco use. As nearly all areca chewers are also tobacco users, the vast majority of patients had the exposure to both factors (1, 2). There were several cell lines arising from OSCC associated with areca chewing/tobacco use or areca nut extract (ANE)/2,4-dimethylbenzoic acid (DMBA) application being established (3, 4). These cell lines have become valuable in understanding the molecular pathogenesis of OSCC. Ko et al. (5) have demonstrated that areca chewing is the most potent risk factor for the development of OSCC in Taiwan, although very few areca chewers are non-smokers. Chen et al. (2) have identified in a large-scale survey that around 13% OSCC from Taiwanese were associated with areca chewing without tobacco smoking. To obtain an OSCC cell line with the risk factor exposure to areca chewing is crucial for investigating the pathogenetic roles of areca.

p53, the major guardian of genome, drives a variety of anti-cancer functions of apoptosis and cell cycle arrest in the case of DNA damage, excessive oxidative stress, and mitogenic stimuli (6). p53 regulates its downstream cyclin-dependent kinase inhibitor, p21, for the execution of G1/S and G2/M arrest (6). The functional abrogation of p53 is frequently through mutation, phosphorylation, or binding to oncogenic proteins (7). Around 25–45% areca-associated OSCC carry *p53* mutations (8, 9). Although the frequent p53 alterations identified in OSCC cell lines has enhanced the understanding of interaction between p53 and disease development, OSCC cell lines carrying wild-type p53 is also important to approach the molecular interaction in pathogenetic process (10, 11). In addition, the most common gains of chromosome arms in areca-associated OSCC were 8q and 9q, and the most frequent losses were of chromosomal arms 3p and 4q (1). Identification of areca-associated cell lines with similar karyotypic changes may lead to the understanding of genomic basis of tumorigenesis.

The activity of areca on the induction of oxidative stress, genotoxicity, and mutagenesis has been verified (12–15). Areca also acts as a tumor promoter or synergistic agent in hamster buccal pouch chemical carcinogenesis (4). Nuclear factor κB (NF-κB) gene-regulatory protein plays central roles in cellular survival and apoptosis, responding to

Correspondence: Dr Shu-Chun Lin, PhD, Institute of Oral Biology, School of Dentistry, National Yang-Ming University, Li-Nong St. Sec. 2, No. 155, Peitou, Taipei 112, Taiwan. Tel: +886 2 28267272. Fax: +886 2 28264053. E-mail: sclin@ym.edu.tw
Accepted for publication June 25, 2003

exogenous stimuli (16–20). It can be activated by carcinogens and tumor promoters to bestow advantages for cancer development (16). However, no study has elucidated the modulating effects of ANE on cellular signaling in target cells, which could be the molecular basis of the neoplastic process.

In this study, we reported the establishment of an OSCC cell line, oral carcinoma 3 (OC3), from an areca chewing/non-smoking patient. The preliminary characterizations of growth, p53 status, and karyotypic imbalances were employed. OC3 cells responded to ANE treatment, as reflected by activation of NF-κB. The novel findings might designate the potential of OC3 in exploring the areca-associated pathogenesis.

Materials and methods

Tumor material and culture

A 57-year-old man presented with a rapidly enlarging painful mass on right cheek. He had areca-chewing habit for 30 pack-years. He did not smoke and only drank occasionally. Physical examination revealed a $4.5 \times 4 \times$ 1.3-cm papillary mass admixing with ulcerative regions locating on right buccal mucosa. An incisional biopsy reported a squamous cell carcinoma. CT scan revealed no cervical lymphoadenopathy and the absence of thoracic or abdominal lesion. A wide excision with partial mandibulectomy was performed to remove the primary lesion. The specimen was histologically confirmed an OSCC. The patient underwent post-operative radiation therapy and was followed routinely for 26 months, with no evidence of recurrence. As consented by the patient, an $\sim$1-cm^3 portion of tumor taken from resected specimen and 5 ml of patient's blood was sampled for cell culture and molecular analysis. Approximately 0.5-cm^3 tumor material was chopped into $\sim$0.1-cm^3 cubes. The cubes were then placed in 60-mm dishes with keratinocyte serum free medium (KSFM; Life Tech., Gaithersburg, MD, USA) supplemented with 1% penicillin/streptomycin/mycostatin (Life Tech.) for the first 15 passages culture to eliminate contaminating fibroblasts. The cells were then grew in a medium composed of DMEM containing 10% fetal bovine serum (FBS) and KSFM in a 1 : 2 ratio in the subsequent passages. Normal human oral keratinocyte (NHOK) at 3rd passage was grown in KSFM. Oral epidermoid carcinoma cell Meng-1 (OECM-1) cells were cultured in RPMI1640 medium containing 10% FBS (Life Tech.). The preparation of ANE from ripe areca nut followed the protocols established (4).

Determination of OC3 growth curve

A total of 5×10^3 cells were seeded in a T-25 flask (Nalge Nunc Int., Naperville, IL, USA) and trypsinized at 24-h interval for 8 days. The assessments were conducted in triplicate. The growth curve and the population-doubling time were obtained by counting the mean number of cells at each day. The population-doubling time was obtained by the formula: population-doubling time $= ((T - T_0)\ \log\ 2)/(\log N - \log N_0)$ (4), where the T is the time after inoculation of the cells and N is the average number of cells/mm^2.

Trypan blue dye exclusion assay

Cells were seeded on 6-well plates at a concentration of 5×10^4 per well and culture for 18 h. Cell viability was determined by the ability of cells to exclude 0.5% trypan blue (Biological Industries, Tel Aviv, Israel) following treatment with ANE for 0, 2, 12, and 18 h at 0, 5, 10, and 20 μg/ml. An equal volume of trypan blue dye solution (0.1% w/v), PBS, and cell slurry were combined and allowed to sit for 5 min at room temperature. The cells were scored as vital or dead based on uptake of dye. All measurements were performed in triplicate.

Immunocytochemistry

Cells grown on 6-well chamber slides (Nalge Nunc Int.) were fixed in 3% paraformaldehyde and permeablized with 0.5% Triton in PBS. After blocking non-specific binding with 2% dry milk in PBS, the slides were incubated with primary anti-cytokeratin 14 (Novocastra Laboratory Newcastle, UK) and anti-vimentin (Santa Cruz Biotech, Santa Cruz, CA, USA) at 1 : 200 and 1 : 1000 dilutions, respectively. Horseradish peroxidase-conjugated anti-mouse (Amersham, Piscataway, NJ, USA) secondary antibodies were employed using standard protocols (7). Sections were then treated with aminoethyl carbazol (AEC) chromogen (Zymed, South San Francisco, CA, USA) and 0.01% H_2O_2. The slides were counterstained with hematoxylin before mounting.

Chromosomal analysis

The comparative genomic hybridization (CGH) was performed using the standard protocol (1). Briefly, metaphases of normal peripheral blood mononuclear cells (PBMCs) were prepared according to standard procedures. The genomic DNA of OC3 was labeled with Spectrum Green-dUTP (Vysis, Downers Grove, IL, USA) using BioNick® kit (Life Tech.), whereas reference DNA from peripheral lymphocytes from the same individual was labeled with Spectrum Red-dUTP (Vysis). The labeled DNA was then mixed with unlabeled human Cot-1 DNA (Life Tech.), and dissolved in hybridization solution. The probe mixture and metaphase chromosome were denatured first and mixed for hybridization at 37°C for 3 days. After hybridization and washing, the chromosomes were counterstained with diamidino-2-phenylindole (DAPI). Fluorescence signals from the hybridized chromosomes were captured and analyzed using QUIPS XL genetics workstation system (Vysis). The ratio profile of green (amplification) to red (deletion) fluorescence intensity was plotted as a function of locations along individual chromosomes using the QUIPS software. Data from more than 15 captured metaphases were combined to obtain an averaged ratio profile for each sample. Gain or loss was defined by setting the thresholds at 1.2 and 0.8, respectively (21). The experiments were repeatedly performed to assure the reproducibility.

4q loci analysis

Multiple highly informative loci markers D4S3029 (4q13.1), D4S7517 (4q21.1), D4S414 (4q22.2), D4S407 (4q25), D4S430 (4q27), D4S424 (4q31.22), D4S413 (4q32.1), and D4S1529 (4q34.1) with a $\sim$15 cM in distance were used for alleotyping of 4q. The PCR primer sequences used to amplify the marker segments were obtained from Genome Data Base (GDB), USA (http://www.gdb.org) and Marshfield database (http://research.marshfieldclinic.org/genetics). Ten nanograms of genomic DNA was used as a

Table 1 Primers used for *p53* analysis using RT-PCR

Exon	*Primer name*	*Primer (no. of terminal base)*	*Size of amplicon (bp)*
1–4	1S	5′-aagtctagagccaccgtcca-3′ (78)	499
	1A	5′-gacttggctgtcccagaatg-3′ (576)	
4–6	2S	5′-agaatgccagaggctgctc-3′ (407)	467
	2A	5′-tagggcaccaccacactatg-3′ (873)	
5–9	3S	5′-cacatgacggaggttgtgag-3′ (716)	476
	3A	5′-tctccatccagtggtttcttc-3′ (1191)	
8–11	4S	5′-gcgcacagaggaagagaatc-3′ (1060)	449
	4A	5′-ttctgacgcacacctattgc-3′ (1508)	

template. The amplicons were detected by laser fluorescence on ABI377 auto sequencer (Applied Biosystems, Foster City, CA, USA). Data were analyzed by Genescan analysis and genotyper software (Applied Biosystems). Intensity calculations and comparisons were performed on the amplicons of patient's PBMC DNA and OC3 DNA to evaluate microsatellite instability or allelic deletion.

RT-PCR/cloning and sequencing

Total RNA was isolated and converted to cDNA using reverse transcriptase (Stratagene, La Jolla, CA, USA). The coding sequence of *p53* (1167 bp) was amplified to generate four overlapping segments using primers (Table 1). Aliquots of each amplification reaction were resolved in a 2.5% agarose gel, stained with ethidium bromide, and visualized by image system (Viber Lourmat, Marne La Valle, France). The gel-purified amplicons products were cloned into the pGEM-T vector (Promega, Madison, MA, USA). Plasmid DNA was purified with the use of plasmid mini kits (Qiagen, Valencia, CA, USA). Plasmid DNA of at least five independent clones was subjected to sequencing using T7 vector primer and ABI 377 automatic sequencer (Applied Biosystems). An OSCC cell, OECM-1 cell containing *p53* point mutation, served as a positive control. PCR reaction without template served as a negative control.

Western blot analysis

Cell lysates were resolved by electrophoresis on a 10% denaturing polyacrylamide gel. The protein was electroblotted onto nitrocellulose membranes using a regular blotting system (Hoeffer, San Francisco, CA, USA). The dilution for primary anti-p53 Ab (DO7 from Dako, Carpinteria, CA, USA), anti-p21 Ab (EA10 from Calbiochem, La Jolla, CA, USA), and anti-α-actin Ab (Chemicon) were 1 : 200, 1 : 200, and 1 : 1000, respectively. Horseradish peroxidase-conjugated anti-mouse (Amersham) secondary antibodies were employed using standard protocols (7). Autoradiography signals were detected by a chemoilluminesence detection system (Amersham).

Electrophoretic mobility shift assay (EMSA)

Nuclear extracts were prepared using standard protocol. The protein content was measured by the method of Bradford. EMSA was performed by incubating 8 μg of nuclear extract with 16 fmol of ^{32}P-end-labeled, double-stranded 45-mer NF-κB oligonucleotide in a buffer containing 20 mM 4,(2-hydroxyethyl)-1-piperazineethanesulfonic acid (HEPES) (pH 7.9), 4% Ficoll, 100 mM KCl, 0.2 mM ethylenediamine tetra-acetic acid (EDTA), 0.5 mM phenylmethylsulfonyl fluoride, and 0.5 mM 2,3-dihydroxy-1,4-dithiobutan,1-4-dithiothreitol (DTT) for 30 min at 25°C. Protein–DNA complexes were resolved on a high-ionic strength 4% polyacrylamide gel containing 0.5× Tris-borate EDTA buffer (380 mM glycine, 45 mM Tris base (pH 8.5), 45 nM boric acid, and 2 mM EDTA). The composition and specificity of binding were examined by competition with 100-fold excess of unlabeled oligonucleotide. For the supershift assays, nuclear extracts were incubated with the antibodies (Santa Cruz) against either p65 and/or p50 subunits of NF-κB for 30 min at 37°C before the complex was analyzed by EMSA. The gel was dried after resolution. The radioactive bands from dried gels were quantitated by a phosphorimager (Amersham).

Results

Morphological and growth characteristics

OC3 cells cultivated at 30th passages were defined as early-passage OC3 cells. The characterizations of OC3 cell were performed mainly on stably growing 80th-passage cells, together with early-passage cells in some experiments. The primary tumor composed mainly of larger polymorphic polygonal and scanty smaller ovoid keratinocytes. The tumor cells exhibited nuclear hyperchromatism, prominent nuclei, and frequent mitotic figures (Fig. 1A). Focal areas also contained some keratin pearls, epithelial pearls, and scattered dyskeratotic cells with eminent intercellular bridges. It was diagnosed an OSCC, moderately differentiated. The initial cultivated cells migrated from tissue explants exhibited polygonal or ovoid cellular nests admixed with clusters of spindle cells. The cytokeratin 14 and vimentin expression in cultivated cells was monitored by Western blot every 5 passage to check the cell components. Following the complete extinguish of contaminating fibroblasts under the culture in KSFM for 15 passages, the cells were subcultured to a medium containing DMEM and KSFM at 1 : 2 ratio with a final FBS of 3.3%. The cells were passaged around 90 times, and continued to grow in a monolayer. It was designated the OC3 cell line. OC3 cells exhibited polygonal or ovoid cellular appearance in culture (Fig. 1B) and had cytokeratin 14 accumulation (Fig. 1C), particularly in polygonal cellular fraction. The growth of OC3 cells was at a lag phase in the initial 24 h, followed by days at logarithmic phase. The cells entered a stationary phase on the 8th day. During the logarithmic phase, the population-doubling time of early-passage OC3 cells was 23 h, while it was 16 h in 80th-passage OC3 cells.

Karyotypes and 4q status

The chromosomal analysis using CGH has revealed the amplification in chromosomes 1q32–42, 5q13.2–31.3, and 8q, the deletion in 4q31–35, 6p, 8p, 10p, and 10q11–12 as well as the gain of chromosome 20 in early passage OC3. However, the alterations in chromosome 10 were not detected in 80th-passage cells (Fig. 2A). Except for D4S3029 (4q21) exhibiting homozygosity, the microsatellite analysis showed the loss of heterozygosity at D4S407, D4S430, D4S424, and D4S413 spanning 4q25–4q32 as well as the instability at D4S1517, D4S414, and D4S1529 surrounding the deleted region in the DNA of OC3 cells relative to patient's PBMC DNA (Fig. 2B). In general, the alleotypic

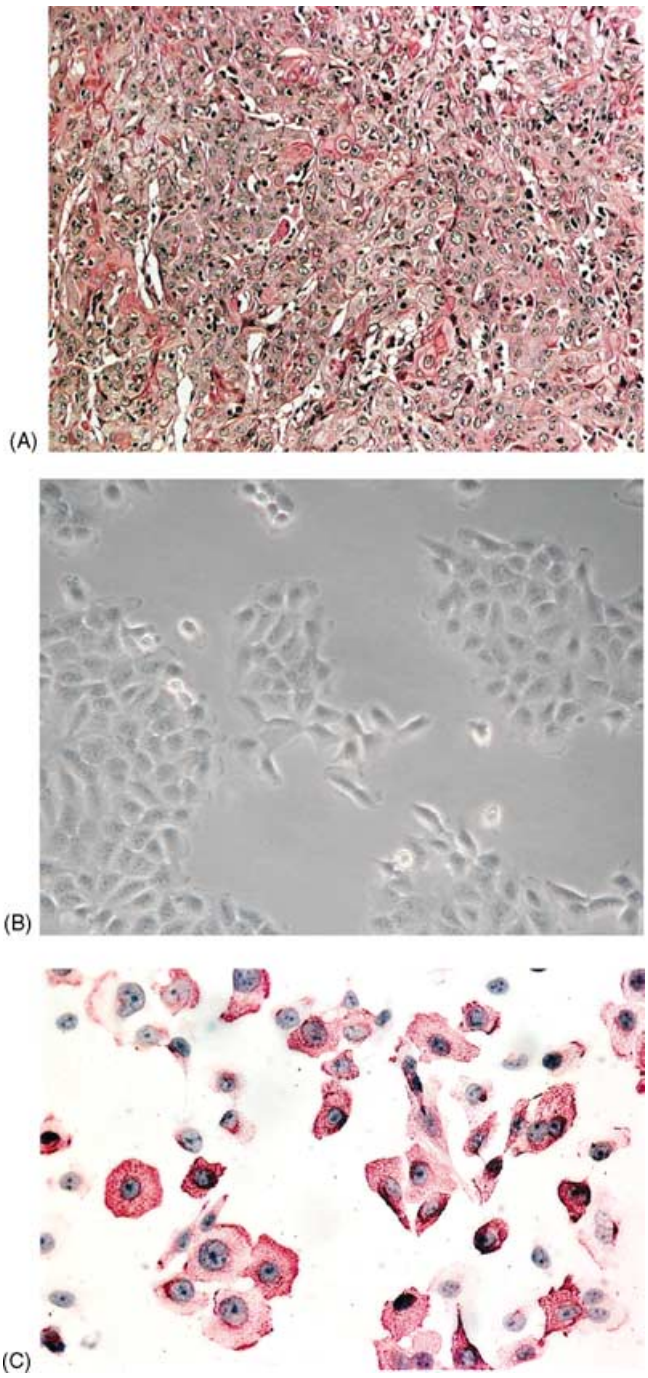

Figure 1 (A) Pathologic examination of primary lesion exhibited a moderately differentiated OSCC composed mainly of polymorphic epithelial cells with prominent nucleoli. Keratinization can be seen in focal areas. (B) OC3 in culture. Note the larger polygonal cells as the major component and some smaller ovoid cells. (C) The cytokeratin 14 expression in OC3 cell. The larger polygonal cells have more intensive cytokeratin 14 expression.

mapping of 4q loci was rather in agreement with the results of karyotypic analysis, suggesting the long-spanning deletion of telomeric part of 4q in OC3 cells.

p53 status

Amplification of the cDNA from OC3 cells generated amplicons encompassing coding sequence (base # 215–1396) and the vast majority of 5′-untranslated region (UTR) (base # 78–214) and 3′-UTR (base # 1397–1508). The mixtures of multiple PCR reactions were cloned and sequenced bi-directionally using T7 and SP6 promoter primers. A G → C substitution at base # 171 and 1409 was found both in OC3 and OECM-1. As they were localized in UTR, these substitutions were presumably ineffective to *p53* transcription. In addition, C → G and A → G substitutions were also identified in base # 429 and # 1032 in both OC3 and OECM-1, causing no changes in amino acid sequence. They were interpreted as genetic polymorphism. No other point mutation in *p53* coding sequence was identified in OC3. However, in exon 5, a G to T transversion at codon 173 (GTG to TTG, Val to Leu) was repeatedly found by sequencing of OECM-1 cDNA (Fig. 3A). The Western blot showed that OC3 had profound p53 expression similar to that in OECM-1 and a slight p21 expression similar to that in normal human oral keratinocyte (NHOK; Fig. 3B). The early-passage OC3 cells had p53 and p21 expression level similar to those in 80th-passage cells (detailed analysis not shown).

NF-κB activation following ANE treatment

Less than 20 μg/ml ANE treatment for 2 h caused no loss of cell vitality. Less than 10 μg/ml ANE treatment for <18 h reduced the viable OC3 cells for <10%. However, 20 μg/ml ANE treatment for 18 h reduced the viable OC3 cells for ∼50% (Fig. 4). The activation of NF-κB associated with ANE treatment with different time periods and dosages was assayed. Figure 5 shows the presence of a major complex, which bind NF-κB probe in control OC3 cell extracts (lane 2), while this complex was not seen in negative control (lane 1), which consisted of only labeled probe in reaction. Ten and 20 μg/ml ANE treatment for 2 h up-regulates the NF-κB binding activity for ∼1.8- and ∼2.7-folds, respectively (lanes 2–4). The treatment for 18 h also up-regulates NF-κB binding activity for ∼1.5-folds (lanes 5 and 6). The specificity of NF-κB binding activities was confirmed by competitive inhibition with an excessive unlabeled probe (lane 7) and supershifts of NF-κB binding complex by conjugating with anti-p65 and anti-p50 antibodies (lanes 8–10).

Discussion

The pathogenetic mechanisms of areca for oral keratinocytes are obscure. Cell lines of OSCC associated with areca exposure are useful for deducing the pathogenetic mechanisms. By literature search, no OSCC cell line associated with such etiologic background has been established. We therefore established a new cell line, OC3, associated with history of areca chewing/non-smoking, to accommodate prospective studies. OC3 cells possess morphologic features of keratinocyte. In addition, they exhibited characteristics of a neoplasm with rapid replication under culture conditions and multiple genomic imbalances. It is likely that two subfractions of OC3 existed. The major one exhibited polygonal morphology and larger size, exhibiting strong cytokeratin 14 expression (a basal-low stratum spinosum keratinocyte marker; 22), while the minor one had small ovoid morphology with little cytokeratin 14 expression. An

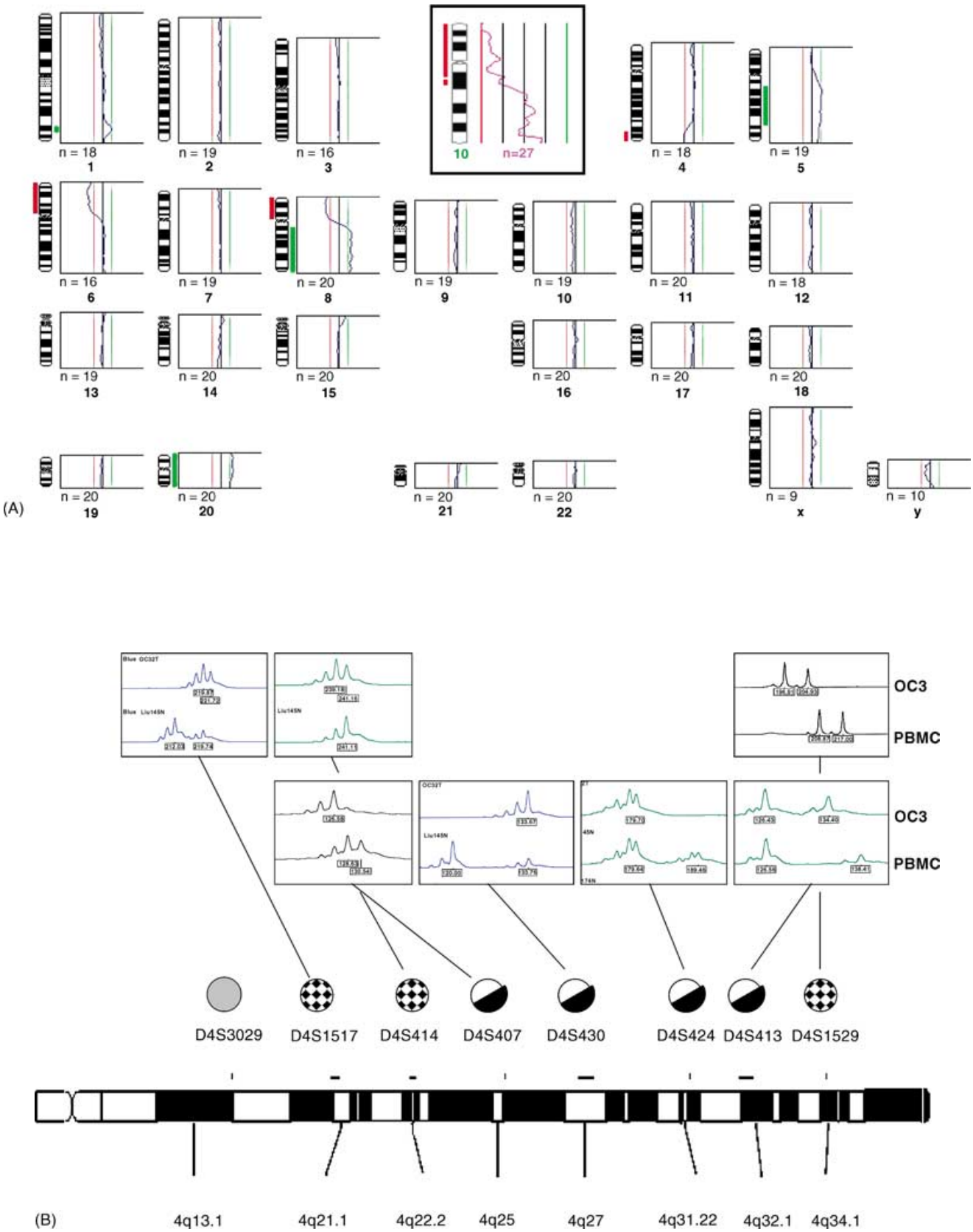

Figure 2 (A) Karyotypic alterations of OC3 at passage 80 detected by CGH (Rt., gain; Lt., loss). Note the alterations in 1q, 4q, 5q, 6p, 8, and 20. The indent shows the CGH karyotyping of early passage OC3 cells, exhibiting the loss of entire 10p and centromeric region of 10q. (B) The 4q mapping using microsatellite markers exhibited the loss of heterozygosity (◪) from D4S407(4q25) to D4S413(4q32.1) and the microsatellite instability (⊕) in the remained 4q loci. ◯, not informative.

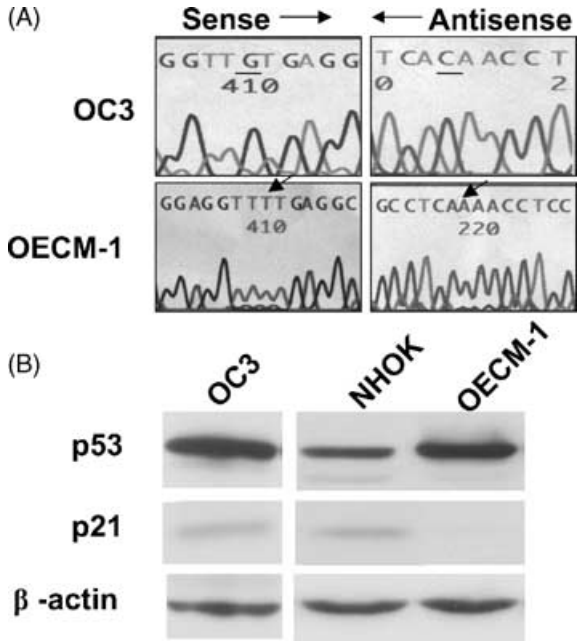

Figure 3 (A) The sequencing analysis revealed the normal *p53* sequence in OC3 compared to a positive control in OECM-1 exhibiting a G → T substitution at codon 173 (GTG to TTG). (B) Western blot showed that OC3 had strong p53 expression and weak p21 expression.

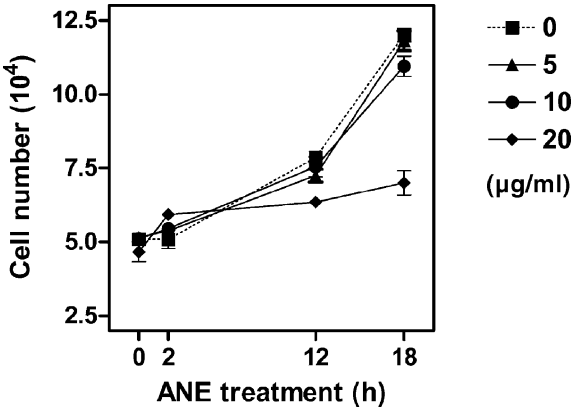

Figure 4 The viability of OC3 cells following the treatment of ANE.

initial attempt to subclone these cell populations was not successful as mutual morphologic transition between these two fractions seemed to occur. Continuous cloning efforts are being laid to obtain more homogenous OC3 cell population.

The patterns of chromosomal imbalances in a tumor might be indicative of certain phenotypic disruption or neoplastic features (21). Chromosomal alterations with gains in 3q, 8q, 9q, 11q, 17q, and 20q and losses in 3p, 4q, 5q, 9p, and 18q appear to be the major karyotypic profile of OSCC (4, 23–25). OC3 cells carry the loss in 4q, gain in 8q, and gain of entire chromosome 20 that are karyotypic changes frequently observed in OSCC. It can be extrapolated for studying the role of these chromosomes in oral carcinogenesis. OC3 cells also carry unique chromosomal gain in 5q and loss in 6p. However, such imbalances, observed only in OC3 cells, were insufficient to implicate pathogenetic significance. Loss of chromosome 4q was detected in ∼50% OSCC (4, 23–26). Hence, it has been implicated to play an important role in the genesis of OSCC (26). The identification of 4q loss as an important prognostic predictor of OSCC in our previous study further highlighted the importance of 4q for OSCC progression (1). Although 4q loss is important for oral carcinogenesis, only few candidate tumor suppressor genes residing have been mapped. The alleotypic analysis employed in this study identified a loss of chromosomal substance from middle to telomeric end of 4q. The regions surrounding the deleted segment also exhibit remarkable instability. The findings might suggest OC3 could be suitable for mapping potential tumor suppressor genes in 4q. It was interesting to note in 80th-passage cells the retrieving of 10p and centromeric 10q chromosomes, which were deleted in the early-passage cells (Fig. 3A). This

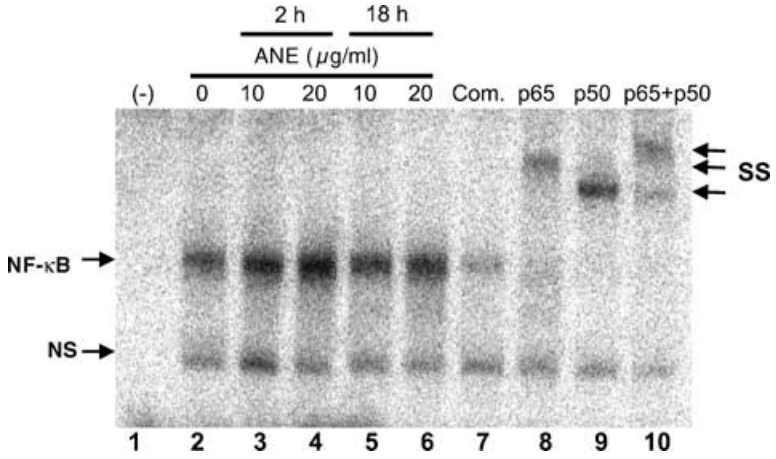

Figure 5 Activation of transcription factors NF-κB in OC3 modulated by ANE using EMSA. Ten micrograms of each nuclear extract was incubated with ^{32}P-labeled probe containing NF-κB in the absence or presence of an excess of unlabeled competitor DNA. Lanes 1, free probe control. Lanes 2–6, treatment of ANE-activated NF-κB at different dosage and time point. Lane 7 contained 100-fold excess of unlabeled probe as competitor DNA to compete the reaction in lane 4. Lanes 8–10, cell lysate was pre-incubated with the antibodies against either p65 and/or p50, followed by standard EMSA. NS, non-specific complex. SS, supershifted complex.

might be caused by the selection of minor cellular population for serial passage *in vitro*. The findings might suggest the requirement of chromosome 10 components for immortalization or proliferation of OC3 in cultivated conditions. There was difference in cell proliferation lying between early-passage OC3 cells and 80th-passage cells. Its association with chromosome 10 deserves further elucidation.

The abrogation of *p53* plays critical roles in carcinogenesis as variable *p53* mutations are commonly found in human tumors. A great majority of OSCC cell lines also carry aberrant p53 protein as a result of gene deletion or point mutation, which could be the genotypic basis of anti-apoptosis, chemoresistance, and angiogenesis advantageous for tumor growth (11, 19, 27). By intensive study, the integrity of *p53* coding sequence in OC3 was verified. Nonetheless, a considerable abundance in p53 protein in OC3 in relation to that in NHOK was also found. Both cells carry similar amount of p21 protein. It appeared that p53 protein was stabilized in OC3 cells. Further elucidation of stabilizing factors including binding to oncogenic proteins, phosphorylation, and acetylation rather than point mutation in OC3 is in progress (6).

NF-κB is the common downstream effector of several signaling pathways (16). Its activation may be indicative for neoplastic process, inflammation, and apoptosis. The repression of NF-κB activity in tumor cell might suppress tumor phenotypes (19), whereas the activation of NF-κB in normal keratinocytes elicits cell cycle arrest (17). The induction of NF-κB activity results in the epithelial hypoplasia, and its blockage induces massive hyperplasia in mice epidermis (18). Thereby, the activation of NF-κB seemed to play contradictory roles in tumor cells versus normal cells. Our EMSA analyses have indicated that ANE can induce the activation of NF-κB in OC3. Such inductive activity was also observed in NHOK under the treatment of non-toxic dosage (data not shown). Elucidation of gene transcription and the accompanied phenotypic changes that are modulated by NF-κB activation in OC3 will certainly bestow toxicogenomic insights of areca.

The OC3 is the first documented OSCC cell line derived from a primary tumor in an areca-chewing patient without exposure to tobacco. It will be an exploratory tool in identification of the pathogenetic impacts of areca through, for instance, the NF-κB pathway.

References

1. Lin SC, Chen YJ, Kao SY, et al. Chromosomal alterations in betel-associated oral squamous cell carcinoma and their relation to clinical parameters. *Oral Oncol* 2002; **38**: 266–73.
2. Chen YK, Huang HC, Lin LM, Lin CC. Primary oral squamous cell carcinoma. an analysis of 703 cases in southern Taiwan. *Oral Oncol* 1999; **35**: 173–9.
3. Wong DY, Chang KW, Chen CF, Chang RC. Characterization of two new cell lines derived from oral cavity human squamous cell carcinomas – OC1 and OC2. *J Oral Maxillofac Surg* 1990; **48**: 385–90.
4. Lin SC, Chang KW, Chang CSYuSY, Chao SY, Wong YK. Establishment and characterization of a cell line (HCDB-1) derived from a hamster buccal pouch carcinoma induced by DMBA and Taiwanese betel quid extract. *Proc Natl Sci Counc ROC* 2000; **24**: 129–35.
5. Ko YC, Huang YL, Lee CH, Chen MJ, Lin LM, Tsai CC. Betel quid chewing, cigarette smoking and alcohol consumption related to oral cancer in Taiwan. *J Oral Pathol Med* 1995; **24**: 450–3.
6. Sharpless NE, DePinho RA. p53: good cop/bad cop. *Cell* 2002; **110**: 9–12.
7. Chang KW, Lin SC, Kwan PC, Wong YK. Association of aberrant p53 and p21 (WAF1) immunoreactivity with the outcome of oral verrucous leukoplakia in Taiwan. *J Oral Pathol Med* 2000; **29**: 56–62.
8. Wong YK, Liu TY, Chang KW, et al. p53 alterations in betel quid- and tobacco-associated oral squamous cell carcinomas from Taiwan. *J Oral Pathol Med* 1998; **27**: 243–8.
9. Hsieh LL, Wang PF, Chen IH, et al. Characteristics of mutations in the p53 gene in oral squamous cell carcinoma associated with betel quid chewing and cigarette smoking in Taiwanese. *Carcinogenesis* 2001; **22**: 1497–503.
10. Chen YJ, Jin YT, Shieh DB, Tsai ST, Wu LW. Molecular characterization of angiogenic properties of human oral squamous cell carcinoma cells. *Oral Oncol* 2002; **38**: 699–705.
11. Noutomi T, Chiba H, Itoh M, Toyota H, Mizuguchi J. Bcl-x(L) confers multi-drug resistance in several squamous cell carcinoma cell lines. *Oral Oncol* 2002; **38**: 41–8.
12. Chen CL, Chi CW, Liu TY. Hydroxyl radical formation and oxidative DNA damage induced by areca quid *in vivo*. *J Toxicol Envir Health A* 2002; **65**: 327–36.
13. Chen CL, Chi CW, Chang KW, Liu TY. The presence of safrole-DNA adducts in betel quid-related oral squamous cell carcinoma in Taiwan. *Carcinogenesis* 1999; **20**: 2331–4.
14. Liu TY, Chen CL, Chi CW. Oxidative damage to DNA induced by areca nut extract. *Mutat Res* 1996; **367**: 25–31.
15. Jeng JH, Chang MC, Hahn LJ. Role of areca nut in betel quid-associated chemical carcinogenesis: current awareness and future perspectives. *Oral Oncol* 2001; **37**: 477–92.
16. Bharti A, Aggarwal B. Nuclear factor-kappa B and cancer: its role in prevention and therapy. *Biochem Pharmacol* 2002; **64**: 883–8.
17. Seitz CS, Deng H, Hinata K, Lin Q, Khavari PA. Nuclear factor κB subunits induce epithelial cell growth arrest. *Cancer Res* 2000; **60**: 4085–92.
18. Seitz CS, Lin Q, Deng H, Khavari PA. Alterations in NF-κB function in transgenic epithelial tissue demonstrate a growth inhibitory role for NF-κB. *Proc Natl Acad Sci USA* 1998; **95**: 2307–12.
19. Li JJ, Cao Y, Young MR, Colburn NH. Induced expression of dominant-negative c-jun downregulates NF-κB and AP-1 target genes and suppresses tumor phenotype in human keratinocytes. *Mol Carcinog* 2000; **29**: 159–69.
20. van Hogerlinden M, Rozell BL, Ahrlund-Richter L, Toftgard R. Squamous cell carcinomas and increased apoptosis in skin with inhibited Rel/nuclear factor-kappaB signaling. *Cancer Res* 1999; **59**: 3299–303.
21. Forozan F, Karhu R, Kononen J, Kallioniemi A, Kallioniemi OP. Genome screening by comparative genomic hybridization. *Trends Genet* 1997; **13**: 405–9.
22. Hansson A, Bloor BK, Haig Y, Morgan PR, Ekstrand J, Grafstrom RC. Expression of keratins in normal, immortalized and malignant oral epithelia in organotypic culture. *Oral Oncol* 2001; **37**: 419–30.
23. Hermsen MA, Joenje H, Arwert F, et al. Assessment of chromosomal gains and losses in oral squamous cell carcinoma by comparative genomic hybridisation. *Oral Oncol* 1997; **33**: 414–8.
24. Okafuji M, Ita M, Hayatsu Y, Shinozaki F, Oga A, Sasaki K. Identification of genetic aberrations in cell lines from oral squamous cell carcinomas by comparative genomic hybridization. *J Oral Pathol Med* 1999; **28**: 241–5.

25. Wolff E, Girod S, Liehr T, et al. Oral squamous cell carcinomas are characterized by a rather uniform pattern of genomic imbalances detected by comparative genomic hybridisation. *Oral Oncol* 1998; **34**: 186–90.
26. Pershouse MA, el-Naggar AK, Hurr K, Lin H, Yung WK, Steck PA. Deletion mapping of chromosome 4 in head and neck squamous cell carcinoma. *Oncogene* 1997; **14**: 369–73.
27. Ji ZW, Oku N, Umeda M, Komori T. Establishment of an oral squamous cell carcinoma cell line (NOS-1) exhibiting amplification of the erbB-1 oncogene and point mutation of p53 tumor suppressor gene: its biological characteristics and animal model of local invasion by orthotopic transplantation of the cell line. *Oral Oncol* 2001; **37**: 386–92.

Acknowledgements

We gratefully acknowledge Suz-Yin Lee, Mei-Fong Chang, Fen-Lin Chen, Shun-Yao Ko, and Dr Ming-Yi Chung for technical assistance. This study was supported by National Science Council grant NSC-91–3112-B-010-003 and National Research Program for Genome Medicine grant 91 GMP 004-3, Taiwan.